

## Polarisation and Angular Correlations of Excited P States of Helium and Hydrogen\*

J. F. Williams

Department of Physics, University of Western Australia,  
Nedlands, W.A. 6009.

### Abstract

The techniques associated with angular and polarisation correlations have been used to study the electron impact excitation of the  $2^1P$  state of helium and the  $2P$  state of hydrogen. The circular, and linear, polarisations of the 58.4 and 121.6 nm radiation have been measured with a double reflection analyser. The measurements have better statistical accuracy than previous work and, for helium at 81.2 eV and a large scattering angle of  $108^\circ$ , confirm that theoretical values are still outside the statistical accuracy of measurement. In hydrogen, the first complete determination of the elements of the  $2P$  density matrix elements is reported. The parameters  $\lambda$ ,  $\text{Re}\langle f_1 f_0^* \rangle$ ,  $\text{Im}\langle f_1 f_0^* \rangle$  and the absolute value of  $\sigma(2p)$  have been measured. No single theory is able to predict the scattering angle dependence above  $70^\circ$ .

### 1. Introduction

Prior to the early 1970s, the experimental study of excited states was generally restricted to the determination of binding energies and lifetimes, the polarisation of the dipole radiation and the total and differential cross sections. Measurements were made with either the photons or the scattered electrons. Fano (1957), Macek and Jaecks (1971) and Fano and Macek (1973) showed how angular or polarisation correlation measurements of the scattered electrons and radiated photons, detected in coincidence, could be interpreted in terms of amplitudes and phases, or equivalently state multipoles or elements of a density matrix. Eminyan *et al.* (1974) showed how the measurements could be made for the  $2^1P$  state of helium. Subsequently many people, for example, Blum and Kleinpoppen (1979), Herman and Hertel (1982) and Andersen *et al.* (1985), have discussed the coherence of the excited states, the symmetry properties of the scattering process, the angular momentum transfer in the collision and the interpretation of the angular, and polarisation, correlations in terms of the shape and orientation of the electron charge cloud of the excited state. The topic has been reviewed most recently by Hanne (1983) and Slevin (1984). The most fundamental advances in the subject have been the measurement of scattering amplitudes and their relative phases as well as the measurement of Stokes parameters,

\* Paper presented at the Specialist Workshop on Excited and Ionised States of Atoms and Molecules, Strathgordon, Tasmania, 3-7 February 1986.

showing the degree of coherence which was complete for the radiation from the magnetic sublevels of the  $3^1P$  state of helium to the  $2^1S$  state.

Those fundamental experimentally derived quantities test the theoretical scattering models for the spin-zero helium scattering before averages over angle or energy are made. Since amplitudes, rather than the moduli squared of the amplitudes, are deduced, the possibility exists of observing interference terms in the density matrix. Recent measurements by Back *et al.* (1984) of the time evolution of the Stark-mixed opposite parity  $2S$  and  $2P$  states of atomic hydrogen attempted to observe such interference terms but were limited by instruments and statistics. Their work has aroused much interest as a first step in determining the total  $n = 2$  density matrix.

Technology in the form of microchannel plates and fast subnanosecond timing electronics has enabled these advances. Microchannel plates, because of their small dimensions and fast electron transit times, respond within  $10^{-9}$  s to incident particles. Their secondary electron emitting surface properties, such as channel electron multipliers, respond to radiation below about 140 nm. Subsequent fast amplifiers, discriminators and coincidence timing maintain coincidence resolving times to less than 1.0 ns. The study of the time development of interfering quantum states has received a new impetus. Also, the microchannel plate is composed of a regular array of sensitive areas each of about 20  $\mu\text{m}$  in diameter and separated by about the same dimension, so that with appropriate sensing of its output, position dependent detection occurs. The subsequent parallel, or simultaneous, rather than serial, detection of particles can be made with an increase in the effective sensitivity of the detector of at least a factor of 100.

The second recent advance is the development of a circular polarisation analyser for 50–200 nm radiation, as used by Williams (1983) and the group of McConkey (e.g. Westerveld *et al.* 1985). The principle was discussed and used by McIlrath (1968). With two gold surfaces rotated at appropriate angles to an incident photon beam, the first reflection introduces a  $\frac{1}{2}\pi$  phase shift and the resultant polarisation is analysed by a second reflection. For a calibrated instrument, two measurements at orthogonal positions of the second reflector yield the circular polarisation. With appropriate positions of the two surfaces, the instrument can be used as a linear polariser as shown by Tan *et al.* (1977).

These advances have enabled new information to be obtained on the  $2^1P$  and  $3^1P$  states of helium and the  $2P$  state of hydrogen, which are now considered separately.

## 2. Theory of the Measurements in Helium

Fig. 1 indicates the experimental geometry for an angular (polarisation) correlation of the scattered electrons and radiated photons from an electron impact excited state. The incident and scattered electron momentum vectors define the  $zx$  plane with the incident electron in the direction of the positive  $z$  axis. The photons are observed in the direction  $n(\theta, \phi)$  and the polarisation vector of the photons lies in the plane of the unit vectors  $\epsilon^{(1)}$  and  $\epsilon^{(2)}$ , where  $\epsilon^{(1)} = (\theta + \frac{1}{2}\pi, \phi)$  is in the plane of  $n$  and  $\epsilon^{(2)}$ , and where  $\epsilon^{(2)} = (\theta, \phi + \frac{1}{2}\pi)$  is normal to  $n$  and  $\epsilon^{(1)}$ . The nature of the photons is given by the Stokes parameters  $I$ ,  $I\eta_1$ ,  $I\eta_2$  and  $I\eta_3$ , where  $I$  is the total intensity in the direction  $n$  and  $I(\beta)$  is the intensity transmitted by a polariser oriented through  $\beta$  relative to  $\epsilon^{(1)}$ , such that

$$I\eta_1 = I(\frac{1}{4}\pi) - I(\frac{3}{4}\pi), \quad I\eta_2 = I(\text{RHC}) - I(\text{LHC}), \quad I\eta_3 = I(0) - I(\frac{1}{2}\pi). \quad (1)$$

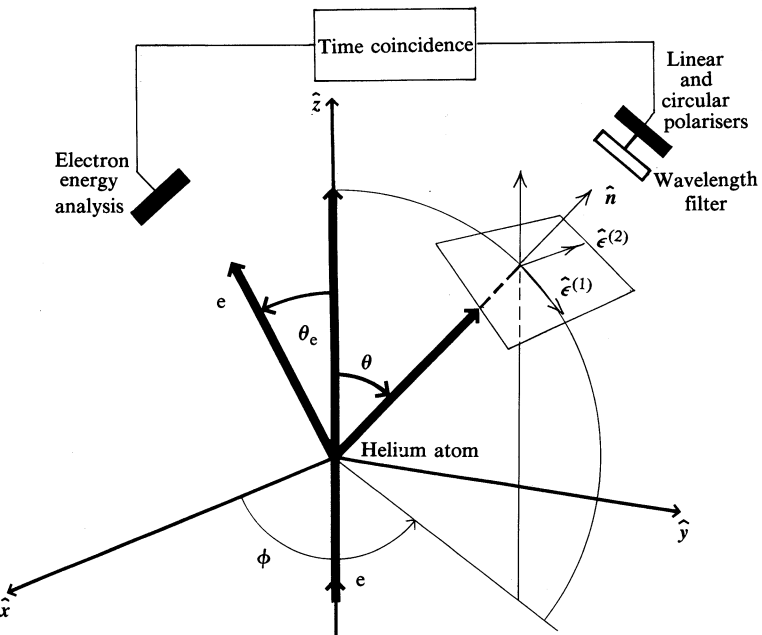


Fig. 1. Right-handed coordinate frame of reference is located by the incident electron beam travelling in the direction of the positive  $z$  axis and the electrons scattered through an angle  $\theta_e$  defining the  $xz$  plane. The photons are emitted in the direction  $n$  with spherical angles  $\theta$  and  $\phi$ . Other features are described in Section 2.

Right-handed circular (RHC) polarisation is defined as a clockwise rotation of the electric vector as observed looking against the direction of propagation of the photons. An alternative notation exists in which  $(\eta_1, \eta_2, \eta_3) = (P_2, -P_3, P_1)$  from classical optics, where LHC photons have positive helicity when the electric vector is seen to rotate counter-clockwise when looking towards the light source.

The degree of polarisation  $P$  of the photons is defined as  $P^2 = \eta_1^2 + \eta_2^2 + \eta_3^2$ , where  $P = 1$  characterises completely coherent photons and  $P < 1$  characterises a statistical mixture of pure states.

Then, for a state  $\psi_i$  excited to a state  $\psi_f$ , the intensity of photons detected by an ideal detector with a solid angle  $d\Omega$  located at  $(\theta, \phi)$  and responding only to a polarisation  $\epsilon$  in a time interval  $t$  to  $t+dt$  is

$$I(\epsilon, \theta, \phi) = \text{const.} |\langle \psi_i | \epsilon \cdot r | \psi_f \rangle|^2 \exp(-\gamma t). \quad (2)$$

The electric dipole matrix element is readily evaluated and the Stokes parameters given in a number of different but equivalent descriptions of a density matrix or multipole moments.

The excitation in helium of  $n^1P$  states from the ground  $1^1S$  state can be described as a coherent superposition of degenerate magnetic sublevels where  $|\psi_f\rangle = f_{+1}|11\rangle + f_0|10\rangle + f_{-1}|1-1\rangle$ , and where  $f_M$  are the amplitudes for exciting the state  $|LM\rangle$ . The elements of the density matrix  $\rho_{MM'}$  are  $\langle LM' | \rho | LM \rangle = f_M f_M^*$  in which the diagonal elements  $\rho_{MM}$  are the differential cross sections  $\sigma_M = \rho_{MM} =$

$|f_M|^2$  and the trace of  $\rho = \sum_M \sigma_M = \sigma$  is the differential cross section summed over all  $M$ .

For  $n^1P$  excitations in helium, symmetry restrictions imply  $f_1 = -f_{-1}$  and three parameters are defined,

$$\sigma = \sigma_0 + 2\sigma_1, \quad \lambda = \sigma_0/\sigma, \quad \cos \chi = \operatorname{Re}(f_0 f_1^*) / \{\frac{1}{2}\lambda(1-\lambda)\}^{\frac{1}{2}}, \quad (3)$$

such that  $\lambda$  and  $\chi$  contain the interference information of the off-diagonal elements of  $\rho$ . Then, equations (1) and (2) give

$$I = C[\frac{1}{2}(1-\lambda)(1 + \cos^2 \theta - \sin^2 \theta \cos 2\phi) + \lambda \sin^2 \theta + \{\lambda(1-\lambda)\}^{\frac{1}{2}} \cos \chi \sin 2\theta \cos \phi], \quad (4a)$$

$$I\eta_1 = C[-(1-\lambda) \cos \theta \sin 2\phi - 2\{\lambda(1-\lambda)\}^{\frac{1}{2}} \cos \chi \sin \theta \sin \phi], \quad (4b)$$

$$I\eta_2 = C[2\{\lambda(1-\lambda)\}^{\frac{1}{2}} \sin \chi \sin \theta \sin \phi], \quad (4c)$$

$$I\eta_3 = -C[\frac{1}{2}(1-\lambda)\{\sin^2 \theta - (1 + \cos^2 \theta) \cos 2\phi\} - \lambda \sin^2 \theta - \{\lambda(1-\lambda)\}^{\frac{1}{2}} \cos \chi \sin 2\theta \cos \phi], \quad (4d)$$

where

$$C = \frac{e^2 \omega^4 d\Omega}{2\pi c^3 \hbar} |\langle 0 \| r \| 1 \rangle|^2 \frac{1}{3} \sigma \exp(-\gamma t).$$

Two different, and equivalent, methods have been used to measure the parameters  $\lambda$  and  $\chi$ . First, angular correlations of the scattered electron and radiated photon, without regard to polarisation, are made at a fixed electron scattering angle  $\theta_e$  by measuring  $I$  as a function of the photon detector angle  $\theta$ . The data are fitted to equation (4a) to yield  $\lambda$  and  $|\chi|$ . The photon detector angle  $\phi$  is usually set at 0 or  $\pi$  to maximise the  $\cos \phi$  term in (4a).

Alternatively, polarisation correlations  $I(\beta)$  are made again for a fixed  $\theta_e$ , usually by fixing the photon detector at  $(\theta, \phi) = (\frac{1}{2}\pi, \frac{1}{2}\pi)$  and rotating the linear and circular polarisers, where

$$I(\beta) = \frac{1}{2} I(1 + \eta_3 \cos 2\beta + \eta_1 \sin 2\beta)$$

and, from (1),  $\lambda = \frac{1}{2}(1 + \eta_3)$  and  $\cos \chi = \frac{1}{2}\{\lambda(1-\lambda)\}^{\frac{1}{2}}\eta_1$  and, since  $\eta_2 = -2\{\lambda(1-\lambda)\}^{\frac{1}{2}} \sin \chi$ , the sign of  $\chi$  can be determined.

Since the  $n^1P - 1^1S$  transitions in helium give rise to 58.4 nm or shorter wavelengths, it is only with the recent development of the double reflection circular polariser that the sign of  $\chi$  could be measured.

### 3. Measurements in Helium

The apparatus, used in similar studies by McAdams and Williams (1982), has been improved by adding multiple photon detectors, as indicated in Fig. 2. For the present work  $D_4$  detected the 501.6 nm  $3^1P - 2^1S$  radiation,  $D_3$  detected the  $n^1P - 1^1S$

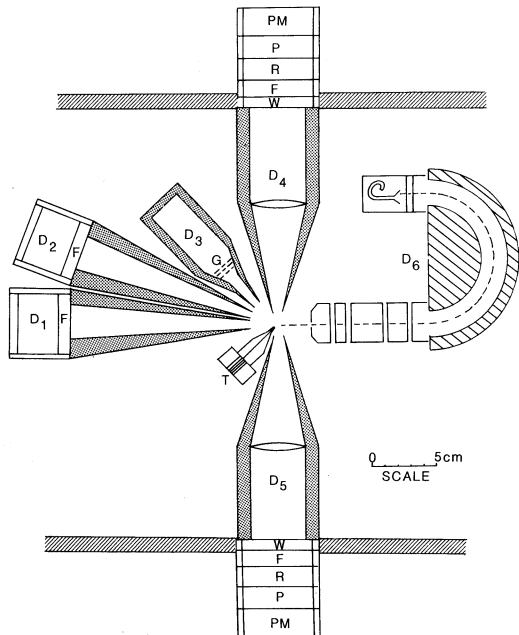


**Fig. 2.** Detector system when the detectors  $D_1$ ,  $D_2$  and  $D_3$  have been rotated into the  $xy$  plane. Detectors  $D_4$  and  $D_6$  lie along the positive  $y$  and  $x$  axes respectively and look towards the origin of coordinates which is the centre of the scattering region. Detector  $D_5$  is the mirror image of  $D_4$ . The incident electron monochromator (not shown) is located along the negative  $z$  axis such that electrons travel out of the plane of the figure. The target atoms effuse from a 200 mm aluminium tube, located in a holder  $T$ , with an exit diameter of 0.3 mm about 1.5 mm from the scattering centre. Detectors  $D_4$  and  $D_5$  consist of a vacuum window  $W$ , filter  $F$ , retarder  $R$ , linear polariser  $P$  and photomultiplier  $PM$  located outside the vacuum system so that it can readily be cooled.

photons,  $D_1$  and  $D_2$  were used occasionally to observe other helium transitions for monitoring purposes, and  $D_5$  was used either as an identical detector to  $D_4$  in early work or subsequently contained a double reflection polariser with a channel electron multiplier detector located wholly within the vacuum system. The reflecting surfaces were rotated manually.

The pulse handling and timing electronics were standard and operated with a coincidence resolving time of about 3 ns. The incident electron beam had an energy resolution of 0.8 eV which was adequate to ensure that the  $2^1P$  and  $3^1P$  states were resolved from other  $n^1P$  states in the scattered energy analyser. The channel electron multipliers detecting the photons responded to all  $n^1P-1^1S$  photons. The  $2^1P-1^1S$  decay was studied at 81.2 eV where there are a large number of previous measurements, and at large angles where there are the largest differences between theory and measurement and the experimental uncertainty is largest. The results are shown in Fig. 3. A single time coincidence spectrum took several days to produce the statistical accuracy shown at  $108^\circ$ . The present circular polarisation values were measured at  $108^\circ$  and  $70^\circ$  (solid triangles in Fig. 3), and they are in reasonable agreement within experimental statistical accuracies with other circular polarisation measurements by Williams (1983) at  $10^\circ$  and  $90^\circ$  (solid squares) and by Khakoo *et al.*

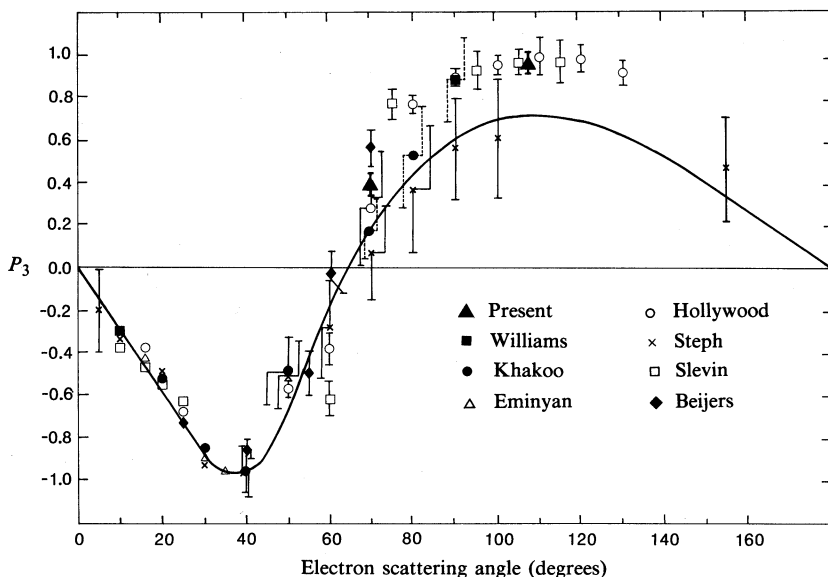


**Fig. 3.** Circular polarisation of the 58.4 nm radiation as a function of the electron scattering angle for an incident electron energy of 81.2 eV in helium, showing the present data at 70° and 108°; Williams (1983) at 10° and 90°; and Khakoo *et al.* (1986). Also shown are experimental values of  $\eta_2$  deduced from the angular correlation measurements of  $|\chi|$  by Eminyan *et al.* (1974); Hollywood *et al.* (1979); Steph and Golden (1980) and Sutcliffe *et al.* (1978); Slevin *et al.* (1980); and Beijers *et al.* (1984). The curve is the theoretical prediction of a distorted-wave theory by Madison and Winters (1983). For clarity, most of the error bars have been deleted at angles below 40°.

(1986) (solid circles). The angular correlation measurements of  $\lambda$  and  $|\chi|$  by a number of workers have been converted to  $P_3$  ( $= -\eta_2$ ) values using the sign of the present values. The largest spread of measured values occurs at electron scattering angles of 60° and 70°, which span the angle (about 63°) at which  $P_3$  changes sign and where its values are changing rapidly. Then the shape of the angular correlation makes the experimental uncertainty large. The error bars shown on the data are plus or minus one standard deviation, which is seen in Fig. 3 for some data to be as large as 0.3 for a quantity  $P_3$  whose value is limited between -1 and +1. The distinguishing feature of the present data is the small experimental uncertainty, which supports the preferred values for  $|\chi|$  to be those of Hollywood *et al.* (1979), and which are strongly supported by the data of Slevin *et al.* (1980). The theoretical distorted-wave calculated values of Madison and Winters (1983) (curve in Fig. 3) are in agreement within experimental uncertainty up to about a scattering angle of 70°, but at higher angles underestimate the measured values.

#### 4. Measurement of the 2P state of Atomic Hydrogen

The second part of this paper concerns scattering from atomic hydrogen, which has always been the preferred atom for study since its wavefunctions are known exactly and any uncertainty in theoretical considerations arises in the scattering approximations. In contrast to helium, the excitation amplitudes are no longer independent of spin and it is a long term aim of this research to measure the spin

dependence of the amplitudes. Also the fine and hyperfine structure modulate the time dependence of the radiative decay, but their effects are either averaged out when the experimental timing resolution is greater than  $10^{-9}$  s or too small to be seen. The scattering amplitudes are the weighted sums of the singlet (S) and triplet (T) scattering amplitudes averaged over the initial spins and summed over the final spins, so that

$$\langle f_M, f_M^* \rangle = \frac{1}{4} \{ 3f_M^S, f_M^{S*} + f_M^T, f_M^{T*} \}.$$

Then, using the approach of Morgan and McDowell (1975), four independent parameters  $\sigma$ ,  $\lambda$ ,  $R$  and  $I$  can be defined:

$$\sigma = \sigma_0 + 2\sigma_1, \quad \lambda = \sigma_0/\sigma,$$

$$R = \text{Re}\langle f_1 f_0^* \rangle / \sigma, \quad I = \text{Im}\langle f_1 f_0^* \rangle / \sigma,$$

which describe the off-diagonal elements of the density matrix but do not yield the relative phase between amplitudes as was possible for helium. A full discussion has been given by Blum and Kleinpoppen (1979) and Slevin (1984). The aim of the present measurements was to completely characterise the excited 2P state, apart from the undetected electron spin.

The present measurements of the  $I$  parameter are a continuation of those by Williams (1983) which were made possible by the development of a double reflection circular polariser. The measurements were made on an apparatus described earlier (Williams 1981) and modified here by the addition of the 121.6 nm polariser and by the use of a microchannel plate as the detector of the energy analysed scattered electrons. By locating this detector along an isochrone, as defined by Volk and Sandner (1983), the electrons passing through the energy analyser were detected with approximately equal flight times. The scattered electron-radiated photon time coincidence spectrum had a resolution of about 3 ns resulting mainly from the use of a channel electron multiplier as the photon detector. Other aspects of the apparatus are unchanged.

Since the apparatus had been completely dismantled since 1981, it was necessary to repeat some of the earlier measurements to obtain values of  $\sigma$ ,  $\lambda$  and  $R$  under identical conditions to those used to measure the  $I$  parameter. It was also necessary to recalibrate the apparatus in an absolute manner. An incident electron energy of 54.4 eV was used because there are considerable data from measurements in the laboratory on the performance of the apparatus as well as a large amount of published theoretical values. Fig. 4 shows normalised angular correlations, i.e. coincidence count rate as a function of photon emission angle, for small ( $10^\circ$ ) and large ( $100^\circ$ ) electron scattering angles. Excellent agreement with previous measurements exists. It is seen that even at a small angle of  $10^\circ$  at 54.4 eV incident energy, there is a significant difference between measurement (curve A) and the first Born approximation (curve B) values. At  $100^\circ$  there are very large differences between theories and measurement. The present work has data points at nine photon angles compared with the previous seven at  $\theta_e = 100^\circ$  and even though the spanned angular range is the same in both cases, there are differences between the values of  $\lambda$  and  $R$  deduced from a least-squares fit to both sets of data depending upon the number of data points used. The values used here have been determined using all nine data points.

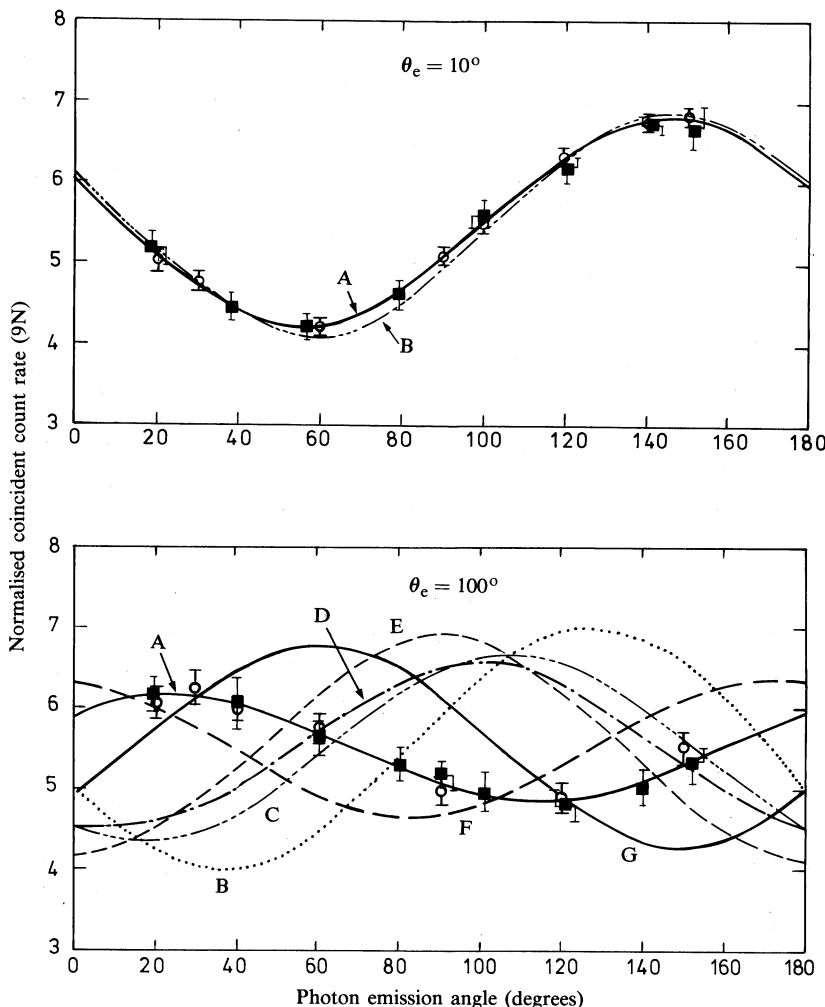


**Fig. 4.** Angular correlation curve, i.e. the variation of the normalised coincidence count rate as a function of the photon emission angle, is shown for an incident electron energy of 54.4 eV and electron scattering angles of  $10^\circ$  and  $100^\circ$ . The present data are shown by squares, while the circles are those by Williams (1981). The full curve (A) is the line-of-best-fit of the angular correlation equation to the data. The other curves are: (B) the first Born approximation, (C) the classical path  $T$ -matrix, (D) the distorted-wave Born approximation, (E) the Glauber approximation, (F) the distorted-wave polarised-orbital approximation and (G) the hybrid close coupling values [see Williams (1981) for reference to theoretical calculations].

Figs 5 and 6 show the  $\lambda$  and  $R$  parameters. Good agreement exists between the various experimental values which are not well described by any of the available theoretical models. A detailed discussion of numerous theoretical models has been given by Bransden *et al.* (1985) in extended coupled-channels calculations. The higher energy reaction channels were included in two ways, namely in either approximate polarisation potentials or normalised square-integrable pseudostates. The values for  $\lambda$  and  $R$  show a shape dependence on  $\theta_e$  similar to the experimental data up to about  $70^\circ$ , but the values are outside the experimental uncertainty although closer than

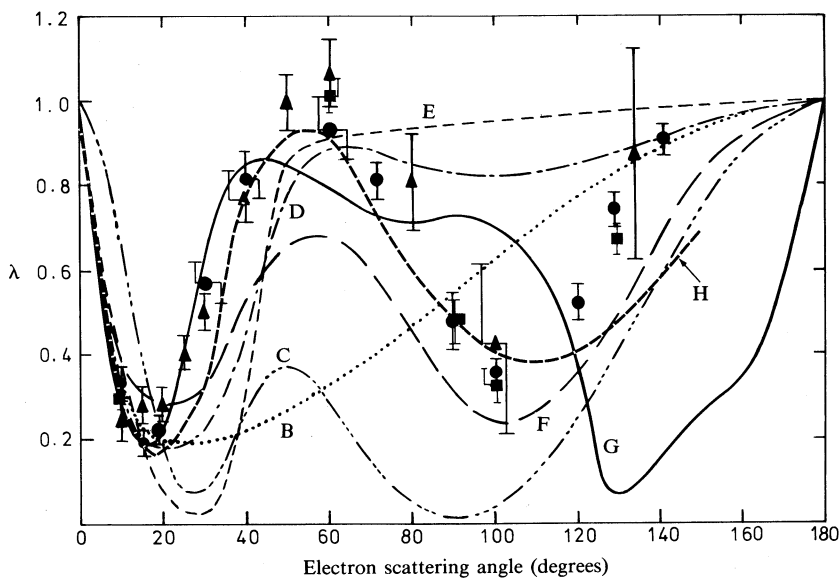


**Fig. 5.** Parameter  $\lambda$  as a function of the electron scattering angle  $\theta_e$  for an incident electron energy of 54.4 eV. The present data are shown by squares and the earlier experimental data are: circles, Williams (1981); triangles, Weigold *et al.* (1980). The theoretical curves (B–G) are the same as in Fig. 4 and also shown (curve H) is the coupled-channels calculation with pseudostate values (PPZ) by Bransden *et al.* (1985).

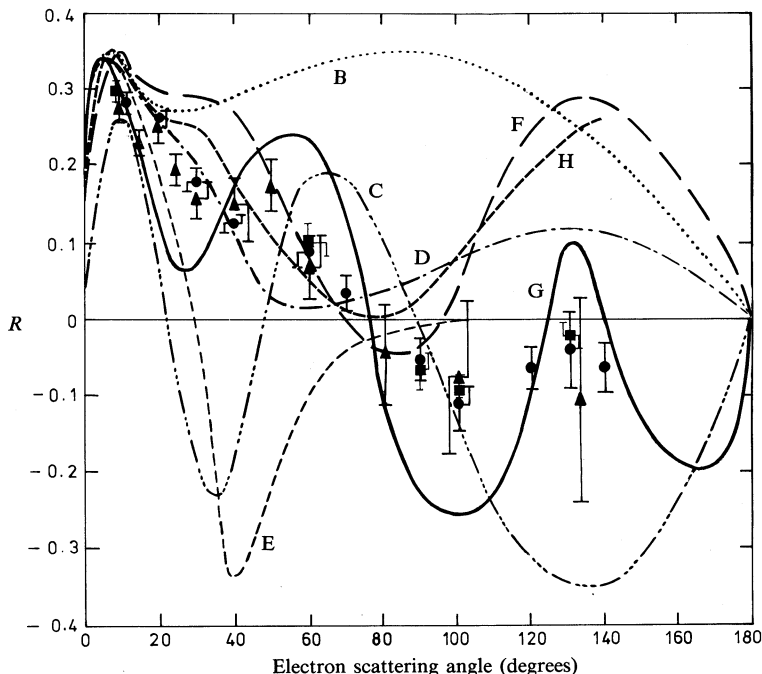


**Fig. 6.** Parameter  $R$  as a function of the electron scattering angle  $\theta_e$  for an incident electron energy of 54.4 eV. The experimental data and the curves are the same as for Fig. 4.

other approximations. None of the eight theoretical models discussed by Bransden *et al.* predicts the negative values of  $R$  for  $\theta_e$  above  $80^\circ$  and, while several models predict good agreement up to  $70^\circ$  with either  $\lambda$  or  $R$ , no one method gives the best agreement with measurement for both  $\lambda$  and  $R$ .

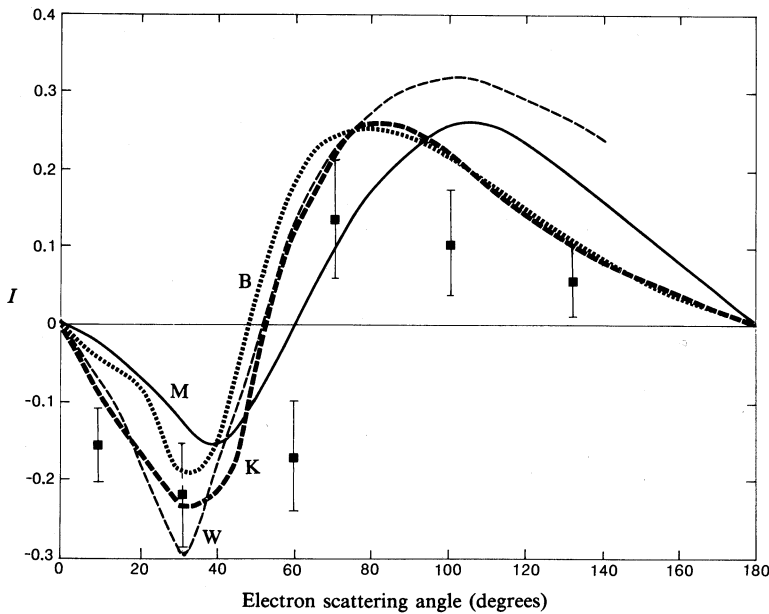


Fig. 7. Parameter  $I$  as a function of the electron scattering angle  $\theta_e$  for an incident electron energy of 54.4 eV. The present data are shown by squares. The theoretical predictions are those by Kingston *et al.* (1982) [K] using the 1s-2p close coupling approximation, by Morgan and McDowell (1975) [M] and by Wyngaarden and Walters (1985) [W] in a distorted-wave polarised-orbital approximation and by Bransden *et al.* (1982) [B] using a second order optical potential model.

Fig. 7 shows the first measurements of the  $I$  parameter. Although the experimental uncertainty (one standard deviation) is large, the measurements show the same general shape as the theoretical predictions. The interesting feature is that a similar general shape agreement exists with the predicted values by Bransden *et al.* (1982) in a model which gave poor values of  $\lambda$  and  $R$ . Subsequent published work by Bransden *et al.* (1985) with improved pseudostates did not include values for the  $I$  parameter—the reader is referred to that paper for a discussion of their theoretical models and for a detailed comparison of predicted values with measured values, not only for  $\lambda$  and  $R$ , but also for  $\sigma(2s)$ ,  $\sigma(2p)$ ,  $\sigma(2s+2p)$  and the elastic scattering cross section. These quantities were measured in previous work (Williams 1981) and have been measured again in the present work, which required an absolute recalibration of the apparatus. The agreement is within 10% for all quantities so the present measured values are not given here. The above measurements completely determine the density matrix elements for excitation of the 2P state.

## 5. Stark-mixed 2S and 2P States

The next step in completely describing the  $n = 2$  state excitation is to measure the interference between the S- and P-state excitation amplitudes; that is, the off-diagonal elements of the  $n = 2$  density matrix given by

$$\rho = \begin{pmatrix} \langle |f_{00}|^2 \rangle & \langle f_{00} f_{11}^* \rangle & \langle f_{00} f_{10}^* \rangle & \langle f_{00} f_{1-1}^* \rangle \\ \langle f_{11} f_{00}^* \rangle & \langle |f_{11}|^2 \rangle & \langle f_{11} f_{10}^* \rangle & \langle f_{11} f_{1-1}^* \rangle \\ \langle f_{10} f_{00}^* \rangle & \langle f_{10} f_{11}^* \rangle & \langle |f_{10}|^2 \rangle & \langle f_{10} f_{1-1}^* \rangle \\ \langle f_{1-1} f_{00}^* \rangle & \langle f_{1-1} f_{11}^* \rangle & \langle f_{1-1} f_{10}^* \rangle & \langle |f_{1-1}|^2 \rangle \end{pmatrix}.$$

A full description of the problem has been given by Blum and Kleinpoppen (1979) and Slevin (1984). Considerable interest exists in the measurement which requires the observation of the initial coherence between states of opposite parity in the presence of an external field to mix the states. At an electric field strength of  $250 \text{ V cm}^{-1}$  the radiative decay should be modulated at periods of about 0.1 and 0.6 ns, corresponding to interference between the fine structure  $P_{1/2}$  and  $P_{3/2}$  states and the Lamb shift states respectively. The first attempts at this measurement using a timing resolution of about 0.5 ns by Back *et al.* (1984) showed the presence of beat structure but the statistics were insufficient to analyse the sinusoidal composition and hence determine the  $\langle f_{1m} f_{00}^* \rangle$  matrix elements. Such measurements using a Stokes parameter determination and the development of a quantitative model have been in progress in Perth for some time.

## Acknowledgments

This work was supported by the Australian Research Grants Scheme and by the University of Western Australia. The measurements would not have been possible without the continuing support of an excellent mechanical workshop, electronics technicians and several honours students. The collaboration with Dr Lydia Heck on the theory of the measurements has been most helpful.

## References

- Andersen, N., Gallagher, J., and Hertel, I. V. (1985). 14th Int. Conf. on Physics of Electronic and Atomic Collisions (Eds D. C. Lorents *et al.*), pp. 57–76 (North-Holland: Amsterdam).
- Back, C. G., Watkin, S., Emelian, M., Rubin, K., Slevin, J., and Woolsey, J. M. (1984). *J. Phys. B* **17**, 2695–706.
- Beijers, J. T. M., van Eck, J., and Heideman, H. G. M. (1984). *J. Phys. B* **17**, L265–9.
- Blum, K., and Kleinpoppen, H. (1979). *Phys. Rep.* **52**, 203–61.
- Bransden, B. H., McCarthy, I. E., Mitroy, J. D., and Stelbovics, A. T. (1985). *Phys. Rev. A* **32**, 166–75.
- Bransden, B. H., Scott, T., Shingal, R., and Roychoudhury, R. K. (1982). *J. Phys. B* **15**, 4605–16.
- Emelian, M., MacAdam, K. B., Slevin, J., and Kleinpoppen, H. (1974). *J. Phys. B* **7**, 1519–42.
- Fano, U. (1957). *Rev. Mod. Phys.* **29**, 74–96.
- Fano, U., and Macek, J. H. (1973). *Rev. Mod. Phys.* **45**, 553–73.
- Hanne, G. F. (1983). *Phys. Rep.* **95**, 97–165.
- Hermann, H. W., and Hertel, I. V. (1982). *Comments At. Mol. Phys.* **12**, 61–84; 127–48.
- Hollywood, M. T., Crowe, A., and Williams, J. F. (1979). *J. Phys. B* **12**, 819–34.
- Khakoo, M. A., Becker, K., Forand, J. L., and McConkey, J. W. (1986). *J. Phys. B* **19**, L209–13.

- Kingston, A. E., Liew, Y. C., and Burke, P. G. (1982). *J. Phys. B* **15**, 2755–66.
- McAdams, R., and Williams, J. F. (1982). *Aust. J. Phys.* **35**, 513–20.
- Macek, J. H., and Jaecks, D. (1971). *Phys. Rev. A* **4**, 2288–300.
- McIlrath, T. J. (1968). *J. Opt. Soc. Am.* **58**, 506–10.
- Madison, D., and Winters, K. H. (1983). *J. Phys. B* **16**, 4437–50.
- Morgan, L. A., and McDowell, M. R. C. (1975). *J. Phys. B* **8**, 1073–81.
- Slevin, J. (1984). *Rep. Prog. Phys.* **47**, 461–512.
- Slevin, J., Porter, H. Q., Emelian, M., Defrance, A., and Vassilev, G. (1980). *J. Phys. B* **13**, 3009–21.
- Steph, N. C., and Golden, D. E. (1980). *Phys. Rev. A* **21**, 1848–55.
- Sutcliffe, V. C., Haddad, G. N., Steph, N. C., and Golden, D. E. (1978). *Phys. Rev. A* **17**, 100–7.
- Tan, K. H., Fryar, J., Farago, P. S., and McConkey, J. W. (1977). *J. Phys. B* **10**, 1073–82.
- Volkel, M., and Sandner, W. (1983). *J. Phys. E* **16**, 456–62.
- Weigold, E., Frost, L., and Nygaard, K. J. (1980). *Phys. Rev. A* **21**, 1950–4.
- Westerveld, W. B., Becker, K., Zetner, P. W., Corr, J. J., and McConkey, J. W. (1985). *Appl. Opt.* **24**, 2256–62.
- Williams, J. F. (1981). *J. Phys. B* **14**, 1197–218.
- Williams, J. F. (1983). 13th Int. Conf. on Physics of Electronic and Atomic Collisions (Eds J. Eichler *et al.*), p. 132 (North-Holland: Amsterdam).
- Wyngaarden, W. L., and Walters, H. R. J. (1985). *J. Phys. B* **18**, L689–94.

Manuscript received 28 April, accepted 23 May 1986